Quantitative analysis of the major components of coal ash by laser induced breakdown spectroscopy coupled with wavelet neural network (WNN)

Jiao Wei,[a] Juan Dong,[a] Tianlong Zhang,[a] Zhanmei Wang,[a] and Hua Li[*a,b]

[a]Institute of Analytical Science, College of Chemistry & Material Science, Northwest University, Xi'an 710069, China

[b]College of Chemistry and Chemical Engineering, Xi'an Shiyou University, Xi'an 710065, China.

Author to whom correspondence should be addressed:

Dr. Hua Li

E-mail: huali@nwu.edu.cn.

Abstract

Laser induced breakdown spectroscopy (LIBS) technique was applied to detecting the major components of coal ash based on wavelet neural network (WNN). Prior to construct the WNN model, the spectra were preprocessed by Wavelet threshold de-noising and Kalman filtering, and the principle components (PC) extracted by principle component analysis (PCA) were used as input variable. Afterwards, the quantitative analysis of the major components in coal ash samples was completed by WNN with the optimized WNN model parameters consist of the number of hidden neurons (NHN), the number of iterations (NI), the learning rate (LR) and the momentum based on the root mean square error (RMSE). Finally, artificial neural network (ANN) and WNN were evaluated comparatively on their ability to predict the content of major components of test coal ash samples in terms of correlation coefficient(R) and RMSE, demonstrating that LIBS combined with WNN model exhibited better prediction for coal ash, and is a promising technique for combustion process control even in online mode.

Keywords: Laser induced breakdown spectroscopy; coal ash; wavelet neural network

1. Introduction

Boiler slag is one of the main factors affecting safe operation of boiler. However, coal ash composition, which refers to the metal and nonmetal oxides and salts generated from various minerals in coal combustion, is an important parameter determining slagging characteristics.[1-2] The composition of ashes depends on the coal quality and the combustion procedure. Therefore, fast and accurate measurement of ash content can judge the trend of the boiling coal slagging, and it is conducive to take measures to prevent or reduce heating surface slagging and to realize the boiling coal ash composition on-line detection. In addition, coal ash was used as partial replacement of cement to product concrete due to its advantages of high production and low cost. It also can be used as soil conditioner and fertilizer, artificial marbles, light aggregates, fine ceramics and so on.[3-5]

Traditional method for the detection of major components include chemical analysis method, X-ray fluorescence, X-ray powder diffraction, inductively coupled plasma atomic emission spectrometry (ICP-AES) and atomic absorption spectrometry (AAS), and so on[6-9]. Nevertheless, these techniques require much time, costly instrumentation and complex sample preparation, thus are not suitable to fast analysis. The prompt gamma neutron activation analysis (PGNAA)[10] is based on the measurement of gamma rays produced by the main constituents of the mineral matter in coal, and has been applied effectively for on-line elemental analysis and proximate analysis of coal. But PGNAA technique has strict regulatory requirements and requires a big amount of samples, and its neutron source presents potential health hazards.

Laser induced breakdown spectroscopy (LIBS) can be described as a rapid, multi-elemental and promising technique with a lot of advantages, mainly including minimal or no sample preparation and destruction, low time consumption and on-line analysis.[11-12] It is an atomic emission spectroscopy technique based on the analysis of spectral lines emitted from the laser-induced plasma, which is obtained by focusing a pulsed laser bean on to a sample. It has been widely applied in industrial processes, environmental testing and geologic exploration, as well as many other fields.[13-17] This technique is first introduced into the on-line detection of coal field, which focuses on the qualitative and quantitative analysis of element composition of fly ash and fluidized coal particles, by Otesen.ect in 1991.[18] In recent years, LIBS technique has been widely used in coal and fly ash. Mateo *et al*.[19] analyzed the influence of accessory elements in coal with different laser wavelengths and sample placements in measurement procedures. As a result, the short wavelength laser is more conducive to accurate measurement. But the accuracy of the repeated measurement needs to be improved. Feng *et al*.[20] used partial least squares (PLS) to solve the problem of low accuracy of coal quality components, and to some extent, improved measurement accuracy. In addition, LIBS combined with PLS has been carried out to extract coal ash content information from LIBS spectra with the motivation of developing an alternative calibration method for accurate and reliable quantitative analysis of ash content in coal by Yao *et al.*[13]. However, it has poor nonlinear fitting ability and tolerance faults. Therefore, a method with well nonlinear fitting capability, tolerance faults, self-organized learning and self-adaptivity was necessary to be proposed for the coal ash analysis. The neural network has the accurate mapping ability to the non-linear problem, however, the traditional artificial neural network[21] has slow convergence rate and is prone to fall into local extremum. Wavelet neural network (WNN) is a combination of wavelet analysis and neural network[22-24], and makes full use of the multi-resolution and partial elaboration of wavelet analysis and self-organized learning and adaptive advantage of neural network. It has been widely applied in the solubility measurements of dyes and petroleum industry.[25-27] It shows wavelet network has stronger adaptive capacity, faster convergence speed and higher precision of prediction than traditional artificial neural network.

The objective of this study put forward a method-WNN for accurate and reliable quantitative analysis of ash content of coal. At first, to get accurate and useful LIBS spectra information, the Wavelet threshold denoising and Kalman filtering were applied in data preprocessing. Afterwards, different input variables were used to construct the WNN model. Then the quantitative analysis of the major component in coal ash samples was completed by WNN with the optimized model parameters (the number of hidden neurons (NHN), the number of iterations (NI), the learning rate (LR) and the momentum) based on the root mean square error (RMSE).

2. Experimental details

2.1. Experimental set-up

The LIBS experimental set-up (Fig.1) is composed of laser, beam focusing system, plasma collecting optics, detection and analysis system device. A Q-switch Nd:YAG laser (λ=1064 nm, 10 ns pulse FWHM, 100 mJ/pulse, repetition rate of 5 HZ) was focused with a 50 mm diameter, 100 mm focal length lens to generate the plasma in air atmosphere pressure. The plasma emission was collected in the direction of a 45° angle by an optical fiber to the entrance slit of an Echelle spectrograph Aryelle 200 (LTB, German) coupled to an ICCD camera (iStar, Andor, EU). The spectrograph provides a constant spectral resolution (CSR) of 6000 over a wavelength range 220-800 nm displayable in a single spectrum. In order to obtain the best signal-to-noise ratio, a delay time between the output-triggered signal for the laser and the beginning scan of the spectrometer was set as 1.5 μs with a gate width of 100 μs.

“Insert Fig. 1 Here”

2.2. Coal ash samples and data acquisition

According to the three ash composition for coal certified reference materials (CRMs) (GSB06-2119-2007, GSB06-2121-2007, GSB06-2122-2007), forty five coal ash samples in powder form with a range of element composition were prepared by mixing the seven major reagents (SiO_2, Al_2O_3, Fe_2O_3, CaO, MgO, MnO_2, TiO_2) which reach percent 95%. Table 1 lists the concentration (wt. %) of major component about 45 samples (1-15# for GSB06-2119-2007, 16-30#for GSB06-2121-2007 and 31-45# for GSB06-2122-2007). Each of employed samples was prepared for LIBS analysis separately with KBr binder. At first, 0.35 g KBr was put and flated in a stainless steel mould, followed by the pour of 0.4 g of powdered ash sample. The powder sample was compressed into a pellet with the pressure of 400 Mpa for 5min. During experiments, the pellet was mounted directly on an X-Y-Z manual micrometer stage. Due to shot-to-shot laser fluctuation, thirty laser pulses per location from each sample were accumulated in order to reduce statistical error, and obtained a measured spectrum. Ten different locations were repeated for each sample. So a total of 450 LIBS (45×10) spectra were obtained. To reduce the influence of the sample heterogeneity, ten spectra of a sample at 10 different locations were averaged into an analytical spectrum; finally we got 45 LIBS spectra (45×1).

"Insert Table 1 Here"

2.3. Wavelet neural network (WNN)

WNN is the combination of wavelet theory and neural networks[22-24], the fusion of wavelet decomposition and feed forward neural network. WNN is a new network based on wavelet transformation[27], in which wavelet function is used as node activation function. It has been proposed as a novel universal tool for functional approximation, which shows surprising effectiveness in solving the conventional problems of poor convergence or even divergence encountered in other kinds of neural network. The typical network model with three layers (input, hidden and output layers) of WNN is shown as Fig.2. Here, due to excellent local performance in time-frequency domain, the Morlet wavelet function ψ is used as excitation function of hidden layer nodes instead of the traditional incentive function such as Sigmoid function. The corresponding weights of input layer to hidden layer and hidden layer threshold respectively by the adjustable parameters of wavelet function and translation parameter b is replaced, and usually a linear output layer neurons, it will be hidden layer wavelet scale is linear superposition to form the output. The dilation and translation parameters take the place of the weights of hidden layer and hidden layer threshold, respectively. Generally, output layer is linear neuron, the output can be obtained with the linear superposition of wavelet dilation coefficient. It is assumed to have **p** samples, m is the number of input nodes, the wavelet network output as follows:

$$y^k = \sum_{i=1}^{n} W_i \, \psi \left[\frac{\sum_{j=1}^{m} \omega_{ij} X_j^k - b_i}{a_i} \right]$$

W_i means the weights of wavelet unit i, $(i = 1, 2, \cdots, n)$, n is the amount of intermediate layers, ω_{ij} is the weights connected the input j-th input X_i to the wavelet unit i; a_i and b_i are the dilation and translation parameters, respectively.

"Insert Fig.2 Here"

In the WNN, the Propagation Algorithm is employed, and with the error function, the values of network parameters $(W_i,\ a_i,\ b_i,\ \omega_{ij})$ can be optimized. The error function E is taken as

$$E = \frac{1}{2P}\sum_{k=1}^{p}\left(y^k - Y^k\right)^2$$

Where Y^k and y^k are the experimental and calculated values, respectively.

The training process and procedure of WNN as follows:

a) Initialize the values of dilation factor a_i, translation parameter b_i, and the network connection weights ω_{ij} and W_i with a random initial value nearby zero.

b) Input the learning samples$\{X_j^k\}$, $(k = 1,\ 2, \cdots, p)$ $(j = 1,\ 2, \cdots, m)$, Y^k, p and m;

c) Learning course of WNN. Compute the output values of the model.

d) With the use of steepest descent method, to modify the network parameters.

e) End the course when the error is less than the presumed value or the steps are more than the max training step, otherwise return b).

3 Results and discussion

3.1. LIBS spectra and data pre-processing

In the collected LIBS spectra data, there are bits of interference information caused by noise and other factors. It can be seen from local amplification figure in Fig. 3 that many interference peaks exists around analysis Al. Therefore, to get useful information from large amounts of data and accurate results, the data preprocessing is a significant step for the WNN model.

"Insert Fig.3 Here"

Here two pre-processing methods (Wavelet threshold denosing[28-29] and Kalman filtering[30]) are employed to filter the noise. The performance of the two methods are estimated by the signal to noise ratio (SNR) and peak distortion combined with the spectra of denoising before and after. The peak distortion can be calculated as follows:

$$\Delta \mathrm{H}(\%) = |\mathrm{H_i} - \mathrm{H_o}| / \mathrm{H_o} \times 100$$

Here, $\Delta\mathrm{H}$ represents the peak distortion, $\mathrm{H_i}$, $\mathrm{H_o}$, are the filtered peak intensity and original peak intensity, respectively. In this study, the wavelet basis function db6 with hard threshold is applied, and the optimal wavelet decomposition level is 5.

"Insert Table 2 Here"

Table 2 shows the results of the two denoising methods. It can be concluded that the SNR of analysis line of Al by Wavelet threshold is higher than that by Kalman filtering, and the peak distortion by the wavelet threshold is much lower than the Karman filter, which affect the quantitative analysis. Therefore, the wavelet threshold is selected to filter the noise.

As data preprocessing, input variable is also important for the WNN model. It can affect the convergence rate and the result of quantitative analysis of the neural network. As seen from Fig.3, the most spectra lines of major elements in coal ash are distributed in the range of 200-500 nm, which contains key features of the specific element, so the spectra of the feature band (200-500 nm) can be selected as input variable. Principal component analysis (PCA)[31-32] as a popular data compression method can not only guarantee the accuracy of the input data and reduce the training time, but also can simplify network structure for WNN. The optimal principal component (PC) is obtained based on the variance captured. Table 3 shows the contribution rate of eleven principal components. It can be seen that the variance captured can be up to 99.97%, when the PC is 9. So the nine principle components are selected as input variable for quantitative analysis.

"Insert Table 3 Here"

Here, the full spectra, the feature band and PC are all used as input variables to construct the model. The performances of WNN model with different input variables are investigated by correlation coefficient (R), root mean square error (RMSE) and time. Table 4 list the results of different input variables, It can be seen that the R obtained by the full spectra, feature band and PC are 0.8973, 0.9468 and 0.9850, respectively. They both show better liner relationship than the full spectra. However, the RMSE (0.0354) generated by the PC is smaller than feature band, and take much less training time. This result owed much to the major information extracted accurately from huge LIBS spectra data by PCA. It can eliminate the interference from other information, and improve the robustness and quantitative performance of WNN calibration model. Thus, the extracted components are regarded as the input variable to construct the model for the analysis of ash content.

"Insert Table 4 Here"

3.2. Quantitative analysis of major component of coal ash

Coal ash is a complex sample containing many chemical elements and thus related to LIBS spectra characterized by hundreds of atomic lines. The extracted components are used as the input variable to construct the model for the quantitative analysis of coal ash. The data set was divided into calibration set and prediction set. 36 samples (1-4#, 6-9#, 11-14#, 16-19#, 21-24#, 26-29#, 31-34#, 36-39#, 41-44#) were selected as calibration set for the construction of calibration model and the rest samples (5#, 10#, 15#, 20#, 25#, 30#, 35#, 40#, 45#) was used as prediction set.

Before constructing the WNN model, the WNN model parameters (NHN, NI, LR and the momentum) are need to be optimized by the gradient descent method[33] based on RMSE. Fig.4a shows the RMSE against the number of neurons in the hidden layer for the calibration set. It can be seen that the optimized NHN is 9 based on the minimum RMSE for the calibration set to prevent the over-fitting of the model. The RMSE against different NI, LV and the momentum are also plotted in Fig.4. It can be seen from Fig. 4b that the RMSE decreases sharply when the NI is in the range of 100-200. However, with the increase of the NI, the RMSE decreases gradually. When the NI is 600, the RMSE is the lowest. So the optimum NI is 600. From Fig.4c and Fig.4d, based on the minimum RMSE, the LR and the momentum are selected to be 0.005 and 0.06, respectively. For fair comparison WNN and ANN, the same parameters of ANN were optimized based on RMSE. The NHN, NI, LR and the momentum are 10, 6000, 0.05and 0.9, respectively.

Under the optimized WNN and ANN parameters, the WNN and ANN model were constructed using 36 training samples. The predictive ability of WNN and ANN calibration model for coal ash was validated by 5-folds cross validation (CV). Fig.5 shows the RMSE and R of major component in coal ash by WNN and ANN calibration model. It can be seen that the RMSE of major component obtained by WNN model is lower than that by ANN calibration model. Moreover, the R of major components obtained by WNN model is much larger than ANN. Therefore, the results show that the WNN model for coal ash is better than ANN.

Based on calibrated WNN and ANN model, the quantitative analysis of coal ash was performed. The performance of WNN and ANN model in terms of RMSE and R were shown in Table 5. As it can be seen, the RMSE of major component in coal ash by WNN model is obvious lower than by ANN model and the R of the major components by WNN is higher than ANN. For SiO_2, Al_2O_3, and Fe_2O_3, the two methods show good linear relationship, while the RMSE obtained by WNN is lower than that by ANN. For MnO_2, the R obtained by WNN significantly improved from 0.5815 to 0.9839, MgO and TiO_2 are the same. In addition, the time of WNN model is much less than that of ANN model. Therefore, the WNN model for coal ash samples was superior to the method of ANN on convergence speed and prediction precision.

“Insert Fig.4 Here”

“Insert Fig.5 Here”

“Insert Table 5 Here”

4. Conclusions

In this work, the quantitative analysis of coal ash was completed by means of LIBS technique combined with WNN model. The LIBS spectra were preprocessed by wavelet transform. The extracted principal components by PCA as input variable were used to construct the WNN model, and the optimized number of hidden layer neural, iterations, the learning rate and the momentum were optimized by the gradient descent method based on the RMSE. In terms of RMSE, R and training time, the WNN model for quantitative analysis of coal ash presents a better performance than that of ANN. This work reveals the capability of the WNN in modeling, and it can be concluded that LIBS technique coupled with WNN method based on PCA is a promising and potential approach for combustion process control even in online mode.

5. Acknowledges

The work was supported by the National Major Scientific Instruments and Equipment Development Projects of China(No. 2011YQ030113), National Natural Science Foundation of China (No. 21375105), Research Fund for the Doctoral Program of Higher Education of China (No.20126101110019).

6. References

1. F. Cangialosi, M. Notarnicola, L. Liberti and J. M. Stencel, Sep. Purif. Technol, 2008, **62**, 240-248.
2. K. H. Pedersen, A. D. Jensen, M. S. Skjoth-Rasmussen and K. Dam-Johansen, Prog. Energ Combust. Sci., 2008, **34**, 135-154.

3. R. M. Dilmore and R. D. Neufeld, J. Energ Eng., 2001, **127**, 37-50.

4. N. Kalra, M. C. Jain, H. C. Joshi, R. Choudhary, R. C. Harit, B. K. Vatsa, S. K. Sharma and V. Kumar, Bioresour. Technol., 1998, **64**, 163-167.

5. J. G. Yoo and Y. M. Jo, Fuel Process.Technol., 2003, **81**, 173-186.

6. P. Arikan, A. Zarasiz and N. Efe, Appl. Spectrosc. Rev., 1996, **31**, 167-178.

7. F. E. Huggins, Int. J. Coal Geol., 2002, **50**, 169-214.

8. M. B. Folgueras, R. M. Dı´az, J. Liberta and M. Alonso, Energy Fuels, 2007, **21**, 744-755.

9. R. Gupta, Energy Fuels, 2007, **21**, 451-460.

10. M. Borsaru, M. Biggs, W. Nichols and F. Bos, Appl Radiat Isopotes, 2001, **54**, 335-343.

11. F. J. Fortes and J. J. Laserna, Spectrochim. Acta, Part B, 2010, **65**, 975-990.

12. D. W. Hahn and N. Omenetto, Appl. Spectrosc., 2012, **66**, 347-419.

13. S. Yao, J. Lu, M. Dong, K. Chen, and J. Li, Appl. Spectrosc., 2011, **65**,1196-1201.

14. T. Zhang, L. Liang, K. Wang, H. Tang, X. Yang, Y. Duan and H. Li, J. Anal. At. Spectrom., 2014, **29**, 2323-2329.

15. G. G. de Carvalho, L. C. Nunes, P. F. de Souza, F. J. Krug, T. C. Alegrec and D. Santos, J. Anal. At. Spectrom., 2010, **25**, 803-809.

16. Y. Lu, Y. Li, Y. Wang, S.Wang, Z. Bao and R. Zheng, Spectrochim. Acta, Part B, 2015, **110**, 63-69.

17. N. J. McMillan, R. S. Harmon, F. C. deLucia and A. M. Miziolek, Spectrochim. Acta, Part B, 2007, **62**, 1528-1536.

18. D. K. Ottesen, L. L. Baxter and L. J Radziemski, Energy Fuels, 1991, **5**, 304-312.

19. M. P. Mateo, G. Nicolas, and A. Yanez, Appl. Surf. Sci., 2007, **254**, 868-872.

20. J. Feng, Z. Wang, L. West, Z. Li and W. Ni, Anal. Bioanal. Chem., 2011, **400**, 3261-3271.

21. B Ö zbalci, I. H. Boyaci, A Topcua, C Kadılar, U Tamer, Food Chem. 2013, **136**, 1444–1452.

22. L. Wang, L. Li, W. Qi and H. Yang, Comput Electron Ang, 2009, **69**, 142-148.

23. C. Yang, J. Wang, X. Sheng, S. Lou, Infrared Laser Eng, 2014, **43,** 3807-3812.

24. T. Yuan, Z. Wang, Z. Li, W. Ni, Ana. Chim. Acta,2014, **807**, 29-35

25. R Tabaraki, T Khayamian and A Ensafi, Dyes Pigm., 2007, **73**, 230-238.

26. M. R Balabin, Z. R Safieva and I. E Lomakina, Chemom. Intell. Lab. Syst., 2008, **93**, 58-62.

27. T. Khayamian and M. Esteki, J. Supercrit. Fluids, 2004, **32**, 73-78.

28. X. Wang and Z. Fu, Eng. Appl Artif Intel, 2010, **23**, 862-871.

29. V. D. Hoang, Trends Anal. Chem. 2014, **62**, 144–153.

30. B. Guo, J. Process Control, 2014, **24**, 81-87.

31. Y. He, X. Li and X. Deng, J. Food Eng, 2007, **79**, 1238-1242.

32. Y. Dou, H. Mi, L. Zhao and Y. Ren, Anal Biochem, 2006, **351**, 174-180.

33. Y. H. Zweiri, L. D. Seneviratne, K. Althoefer, Neural Networks, 2005, **18**, 1341-1347.

Captions:

Fig.1 LIBS experimental set-up for coal ash

Fig.2 The WNN structure

Fig.3 The averaged spectrum of the 20# in the range 200-500 nm

Fig.4 Variation of RMSE vs. (a) NHN, (b) NI, (c) LR and (d) different values of momentum

Fig.5 The performance of WNN and ANN calibration model with 5-fold cross-validation

Table 1. The concentration (wt %) of the major components in coal ash samples

Sample number	SiO_2	Al_2O_3	Fe_2O_3	CaO	MgO	MnO_2	TiO_2
1#	15.76	7.30	39.48	18.09	5.87	0.48	0.30
2#	15.42	7.23	39.44	18.06	5.97	0.41	0.29
3#	15.52	7.44	39.75	17.93	6.18	0.47	0.27
4#	15.56	7.37	39.76	18.39	5.98	0.48	0.26
5#	15.95	7.41	39.84	18.09	6.12	0.47	0.27
6#	15.74	7.22	39.83	18.63	9.19	0.45	0.28
7#	15.65	7.35	39.64	18.02	5.99	0.42	0.27
8#	15.43	7.20	39.74	18.16	5.90	0.44	0.22
9#	15.93	7.28	39.18	17.90	6.00	0.48	0.30
10#	15.58	7.39	39.89	18.72	6.29	0.45	0.29
11#	15.94	7.26	39.64	18.69	6.03	0.46	0.25
12#	15.86	7.29	39.58	18.58	5.83	0.48	0.31
13#	15.61	7.37	39.80	18.64	6.08	0.47	0.30
14#	15.56	7.41	39.32	18.74	6.03	0.45	0.22
15#	15.47	7.26	39.51	18.08	6.27	0.46	0.28
16#	37.18	32.73	4.61	10.28	1.16	0.028	1.41
17#	37.73	33.09	4.83	10.68	1.21	0.021	1.38
18#	37.54	32.78	4.73	10.11	1.17	0.016	1.24
19#	37.32	32.46	4.72	11.20	1.19	0.029	1.23
20#	37.93	32.40	4.91	10.94	1.14	0.040	1.39
21#	37.61	32.83	4.67	10.83	1.27	0.024	1.26
22#	37.22	32.70	4.81	11.21	1.07	0.025	1.41
23#	37.36	32.97	4.65	10.84	1.15	0.017	1.31
24#	37.69	32.89	4.84	11.05	1.20	0.020	1.25
25#	37.76	32.98	4.82	10.86	1.18	0.022	1.31
26#	37.34	32.67	4.70	11.09	1.13	0.019	1.38

27#	37.53	32.88	4.81	10.85	1.22	0.021	1.30
28#	37.16	32.99	4.79	11.19	1.16	0.016	1.40
29#	37.56	32.56	4.89	10.93	1.20	0.017	1.32
30#	37.28	32.95	4.76	11.01	1.24	0.026	1.38
31#	47.85	35.86	2.71	3.23	0.64	-	1.28
32#	48.19	36.08	2.88	3.36	0.76	-	1.38
33#	47.87	35.89	2.75	3.27	0.74	-	1.27
34#	47.66	35.85	2.91	3.24	0.72	-	1.36
35#	47.86	35.95	2.86	3.30	0.73	-	1.35
36#	48.28	36.13	2.90	3.19	0.71	-	1.34
37#	48.13	36.00	2.71	3.34	0.75	-	1.27
38#	47.66	35.88	2.85	3.29	0.67	-	1.24
39#	48.22	35.70	2.83	3.39	0.68	-	1.35
40#	47.72	35.95	2.89	3.25	0.72	-	1.20
41#	48.04	35.67	2.84	3.23	0.75	-	1.38
42#	48.01	36.71	2.86	3.24	0.74	-	1.24
43#	47.92	35.91	2.74	3.23	0.71	-	1.35
44#	48.23	35.97	2.73	3.28	0.69	-	1.19
45#	47.68	35.71	2.72	3.25	0.74	-	1.32

Table 2. SNR and peak distortion of different methods

Denoising method	SNR	ΔH (%)
Original spectra	5.37	-
Wavelet threshold	5.51	4.9
Kalman filtering	2.55	54.7

Table 3. The contribution rate of eleven principal components

PC	Contribution (%)	Cumulative contribution (%)
1	90.69	90.69
2	1.45	92.14
3	1.35	93.49
4	1.31	94.80
5	1.08	95.88
6	1.05	96.93
7	1.02	97.95
8	1.01	98.96
9	1.01	99.97
10	0.01	99.98
11	0.00	99.99

Table 4. The result of WNN with different input variables

Input data	R	RMSE	Time(s)
Full spectra	0.8973	0.0854	900
200-500nm	0.9468	0.0535	480
PC	0.9850	0.0354	2

Table 5.The prediction performance of WNN and ANN for coal ash sample

Component	WNN			ANN		
	R	RMSE	Time(s)	R	RMSE	Time(s)
SiO_2	0.9967	0.2591		0.8844	0.6650	
Al_2O_3	0.9979	0.1129		0.9305	0.7678	
Fe_2O_3	0.9992	0.0934		0.9248	0.8867	
CaO	0.9725	0.1672	14	0.9531	0.1970	27
MgO	0.9989	0.0231		0.7706	0.1621	
MnO_2	0.9839	0.0028		0.5815	0.0209	
TiO_2	0.9802	0.0080		0.7694	0.0414	

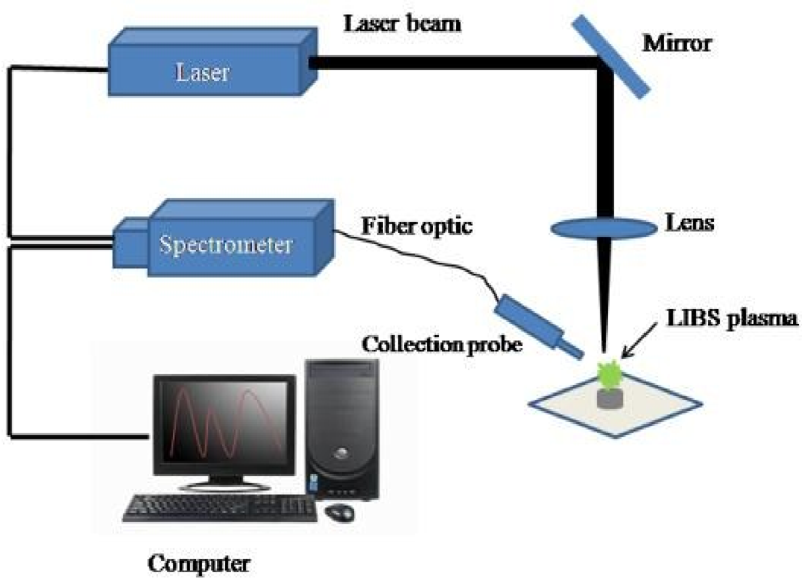
Laser beam
Mirror
Laser
Spectrometer
Fiber optic
Lens
LIBS plasma
Collection probe
Computer

Fig.1

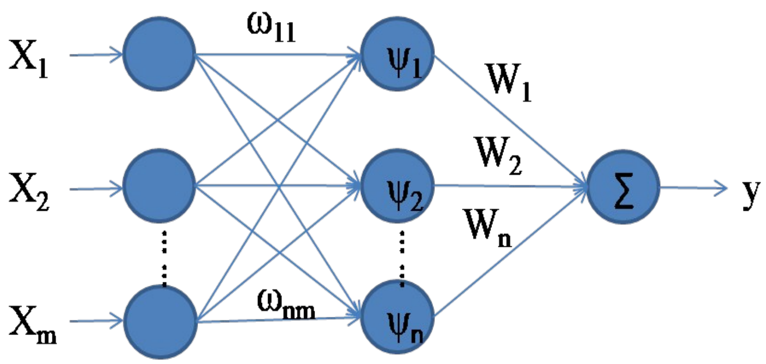
X_1
X_2
X_m
ω_{11}
ω_{nm}
ψ_1
ψ_2
ψ_n
W_1
W_2
W_n
Σ
y

Fig.2

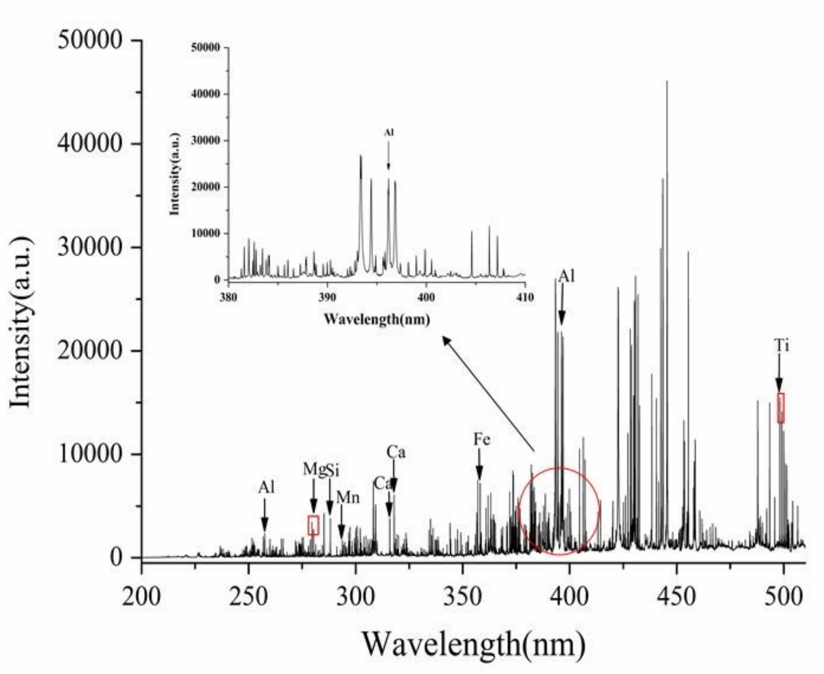

Intensity(a.u.)
Wavelength(nm)
Al
Mg
Si
Mn
Ca
Ca
Fe
Al
Ti
Intensity(a.u.)
Wavelength(nm)
Al

Fig.3

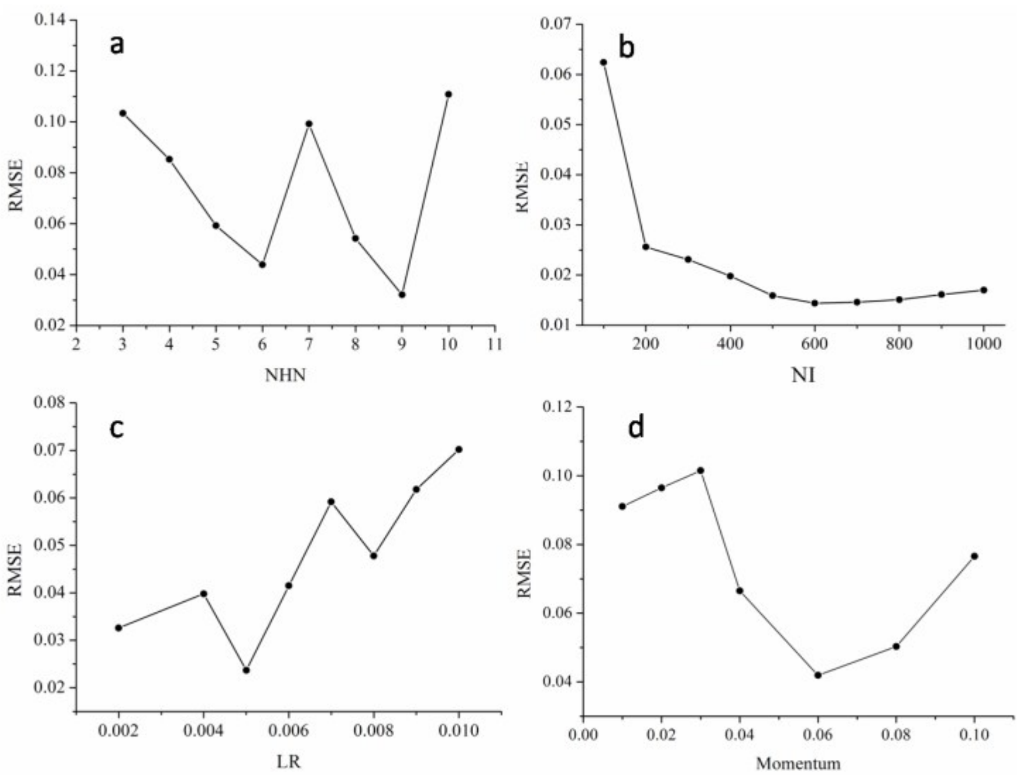

a
b
c
d
RMSE
NHN
NI
LR
Momentum

Fig.4

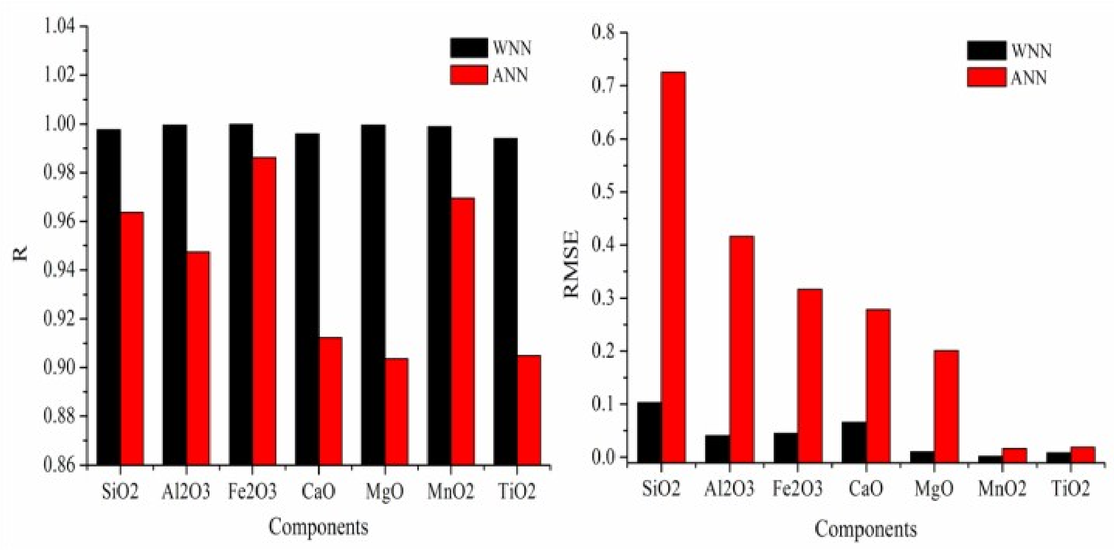
R
1.04
1.02
1.00
0.98
0.96
0.94
0.92
0.90
0.88
0.86
WNN
ANN
SiO2
Al2O3
Fe2O3
CaO
MgO
MnO2
TiO2
Components
RMSE
0.8
0.7
0.6
0.5
0.4
0.3
0.2
0.1
0.0
WNN
ANN
SiO2
Al2O3
Fe2O3
CaO
MgO
MnO2
TiO2
Components

Fig.5

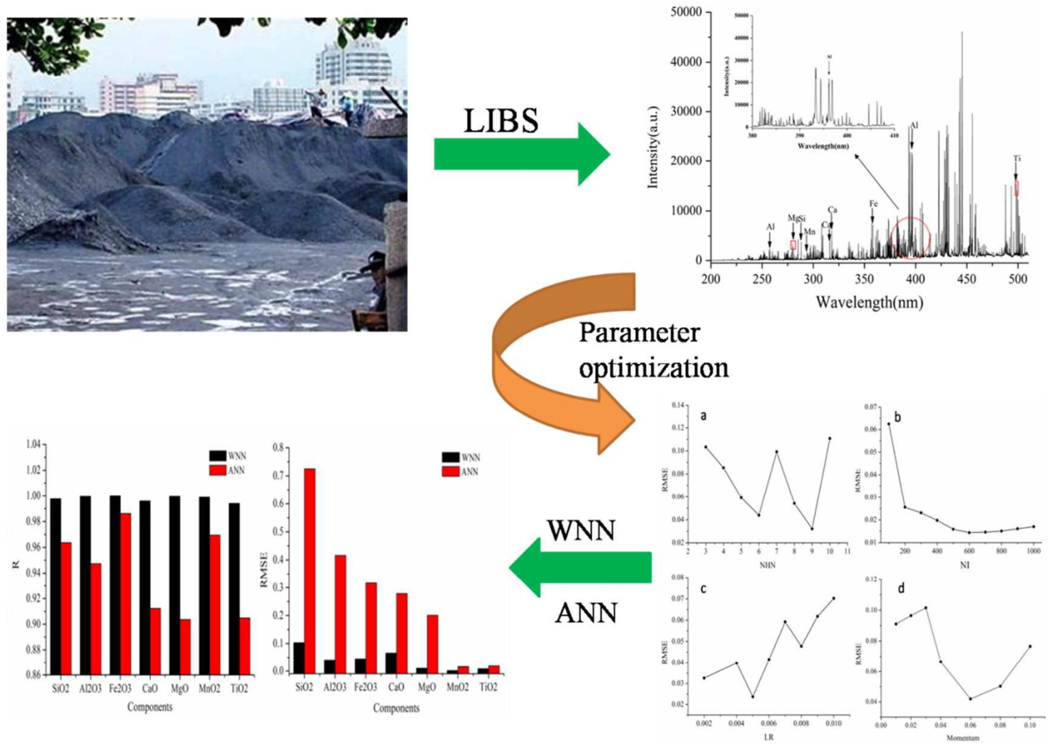

Laser induced breakdown spectroscopy (LIBS) technique combined with wavelet neural network (WNN) was proposed for the quantitative analysis of the major components of coal ash.